JOURNAL OF SOLID STATE CHEMISTRY 88, 70–93 (1990)

Fermi Liquid Behavior and the Metal–Insulator Transition of Almost Localized Electrons: A Brief Theoretical Review and an Application to V_2O_3 System

JOZEF SPAŁEK[1]

Department of Physics and Superconductivity Research Center, Purdue University, West Lafayette, Indiana 47907

Received June 8, 1990

DEDICATED TO J. M. HONIG ON THE OCCASION OF HIS 65TH BIRTHDAY

We review the electronic properties of almost localized electrons and the theoretical interpretation of the observed discontinuous metal–insulator (Mott) transitions in V_2O_3 system, induced by electron–electron interaction. Emphasis is placed on the correlated nature of these electronic states, which are described within a parametrized, Hubbard-type model. In particular, we concentrate on the equilibrium Fermi liquid properties and the Mott transition at nonzero temperature. The effective mass of almost localized quasiparticles is spin dependent and varies strongly in an applied magnetic field. The correlated metal–Mott insulator boundary marks the limiting line of the applicability of the Fermi liquid concept to interacting electrons in a solid. In other words, the insulator to metal (Mott) transitions in V_2O_3 system are regarded as examples of localization–delocalization transformations involving $3d$ electrons. Explicit calculations of the phase diagram are performed with the help of Gutzwiller method and its generalization to nonzero temperatures.

1. Introduction

The electronic properties of solids are usually described in terms of one of the two distinct theoretical schemes: (i) The Bloch–Wilson formulation for extended (band) states and (ii) the atomic approach based on the crystal-field theory and the Heisenberg exchange interactions for quasi-atomic (localized) states of systems with partially filled $3d$ or $4f$ shells. The first is usually applied to ordinary metals and semiconductors, while the latter is appropriate for description of $3d$ or $4f$ states in magnetic insulators and semiconductors. These models and their extensions by perturbation techniques are applicable to a large number of solids. Nonetheless, there exist systems (such as transition metal oxides or rare earth mixed-valence and heavy fermion systems) that exhibit properties intermediate between conventional metals and magnetically ordered insulators. In particular, these are the systems such as V_2O_3, $La_{2-x}Sr_xCuO_4$, $NiS_{2-x}Se_x$, and SmS, in which a transition from the magnetic insulating to metallic state takes place under changes of temperature, of alloy composition, or of pressure. A

[1] Permanent address from October 1, 1990: Institute of Theoretical Physics, Warsaw University, Ul. Hoża 69, PL-00-681 Warszawa, Poland. While at Purdue—on leave from the Department of Solid State Physics, AGH Technical University, Pl-30-059 Kraków, Poland.

0022-4596/90 $3.00

major challenge to theorists has been the development of theories that successfully describe such spectacular discontinuous (magnetic) insulator to metal transitions which do not necessarily involve a change of crystal symmetry. The present understanding of this class of materials starts with the works by Mott (*1*) who emphasized that in the systems like NiO, CoO, and MnO the short-range part of the Coulomb repulsion between the $3d$ electrons may exceed their band energy; the extended (band) states may then be unstable with respect to the localized (atomic like) states. This idea was put on a quantitative basis by Hubbard (*2*) who devised a narrow-band model with short-range (intraatomic) Coulomb repulsion between the electrons. The type of ground state encountered in the Hubbard model depends on the ratio U/W of intraatomic Coulomb repulsion (U) to the so-called bare band width (W). For the systems with $U > W$ the repulsive energy of two $3d$ electrons on the same metallic (M) orbital (e.g., the metal M^- configuration) is larger than the energy ε_k by allowing the electrons to form a band. Thus, the d-shell occupancy remains fixed ($3d^8$ in the case of $Ni^{2+}O^{2-}$) and the material remains insulating even though the spins of $3d$ electrons are free to reorient and the occupancy of $3d$ orbitals does not correspond to a filled band (*3*). Even more important,the $3d$ orbitals remain partially filled even though on the single-particle energy scale they are placed inside the filled oxygen $2p$ band.

Most of the insulators with partially filled $3d$ shells (which are called the Mott insulators) order antiferromagnetically. The modern version of the microscopic mechanism responsible for this magnetic ordering of the Mott insulators has been provided by Anderson (*4*) who introduced the concept of virtual d–d transitions stabilizing the spin singlet configuration of the neighboring pair of cations in second order. This idea of the so-called kinetic exchange is connected with the earlier concept of *superexchange* invoked by Kramers (*5*); in the latter picture the virtual d–d transition is realized via a p–d transition followed by a d–p transition between the magnetic cation and anion (p) orbitals. The kinetic exchange interaction takes place also in strongly correlated metals (*6*), i.e., when the d orbitals on average contain less than one electron per atom and hence the electric transport through the lattice is possible without requiring excitation of the electron across the gap $\sim U$.

Most of the pioneering work concentrated on the nature and the stability of the Mott insulating state at temperature $T = 0$ which replaces the starting metallic state characterized by a half-filled narrow band, when the electron–electron interactions are included. For this purpose two pictures were involved. In the first introduced by Hubbard (*2*) a single half-filled band splits with growing U/W ratio into two (*Hubbard*) subbands and therefore the insulating state is stabilized. The lower Hubbard subband contains half (N) of the total number of states in the starting band which are separated from the upper subband by a gap $E_g \approx U - W$. The transition at temperature $T = 0$ is continuous, as shown schematically in Fig. 1, where the W/U ratio simulates the inverse interatomic separation. At nonzero temperature the system exhibits semiconducting behavior. In this picture the nature of the spin state in the insulating state is not obvious and the empty (hole) states in the lower subbands will behave as itinerant carriers.

An alternative picture of the insulating state has been proposed by Gutzwiller (*7*) and by Brinkman and Rice (*8*). In this picture the mutual balance between the band energy renormalized by the Coulomb repulsion and the interaction part is calculated in a self-consistent way. The latter outbalances the former for $U > U_c \sim W$, and then the electron system reduces to a set of *localized* states. At the metal–insulator transition the electron states transform from

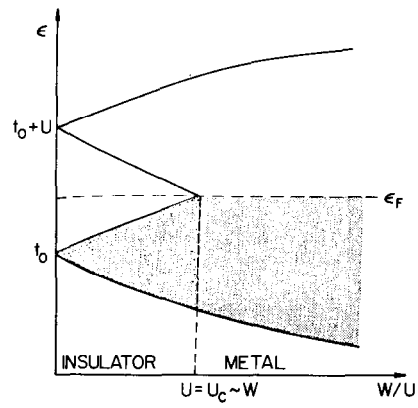

FIG. 1. The Hubbard splitting of the single-particle band states in a half-filled configuration, for the strength of the intraatomic Coulomb interaction $U > U_c$. The filled, lower Hubbard subband for $U > U_c$ represents the Mott insulating state with one electron per atom.

the Bloch-type to the atomic type; i.e., the effective mass of the carriers diverges for $U = U_c$. This picture of the Mott–Hubbard transition can be reformulated in quasiparticle terms (*8–10*) by interpreting the renormalization of the band energy arising from the electron–electron interactions as a band narrowing (or mass enhancement) of the quasiparticle states, as represented schematically in Fig. 2. The quasiparticle picture of the almost localized electrons allows for a generalization to nonzero temperatures and will thus be the principal subject of the present article. We will also include the kinetic exchange interaction in our discussion and then rationalize the whole phase diagram of the systems with metal–insulator transition using pure and doped V_2O_3 as a canonical example of the concepts developed earlier.

2. Groundstate Energy of Correlated Metallic State

In what follows we restrict our discussion to a nondegenerate band whose degree of occupation is described by the average number n of electrons per atom. We consider only the bands half-filled or less-than-half filled, i.e., with $0 \leq n \leq 1$; for a greater band filling ($1 < n \leq 2$) the hole concept may be invoked. We follow the methodology of Ref. (*9*) in writing the band energy of a set of N atomic sites as

$$E_B/N = (t/N) \sum_{i,j(i)\sigma} \langle a_{i\sigma}^{+} a_{j\sigma} \rangle, \qquad (2.1)$$

where $a_{j\sigma}$ is the annihilation operator for an electron with spin σ located in the Wannier state centered on site j which is nearest neighbor to site i, $a_{i\sigma}^{+}$ is the creation operator for an electron of spin σ in the Wannier state located on site i, and t is the transfer integral between sites i and j. The electron–electron repulsion is modeled by the Hubbard type of term.

$$U \sum_i n_{i\uparrow} n_{i\downarrow}, \qquad (2.2)$$

where $n_{i\sigma} \equiv a_{i\sigma}^{+} a_{i\sigma}$ is the particle number operator for occupation of site i by an electron of spin σ and U is the magnitude of Coulomb repulsion for two electrons with

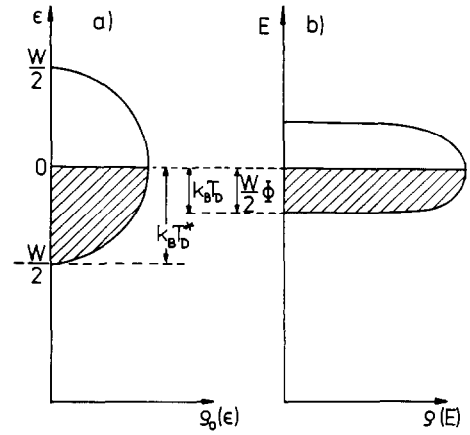

FIG. 2. Schematic representation of bare (ρ^0) and quasiparticle (ρ) densities of states. The band narrowing factor Φ describing the many-body mass enhancement is also specified. The presence of factor Φ relates the degeneracy temperature T_D for quasiparticles to that (T_D^*) for bare electrons via the relation $T_D^* = T_D/\Phi$.

opposite spins and in the same Wannier state.

We consider the situation when the terms (2.1) and (2.2) are comparable; therefore, the expectation value $\langle n_{i\uparrow} n_{i\downarrow}\rangle \equiv \eta$ is regarded as a fundamental parameter which must be determined variationally by calculating the balance between those two terms. For that purpose introduce the total energy E as a sum of (2.1) and the expectation value of (2.2), and then rewrite the sum in the form

$$E/N = \Phi(\eta)\bar{\varepsilon} + U\eta, \tag{2.3}$$

where $\Phi(\eta)$ is a function that describes a restricted motion of particles under the presence of the Coulomb repulsion and is to be determined, and $\bar{\varepsilon}$ is the average bare band energy per atomic site, i.e.,

$$\bar{\varepsilon} = (t/N) \sum_{i,j(i)\sigma} \langle a_{i\sigma}^{+} a_{j\sigma}\rangle \equiv (1/N) \sum_{k<k_F} \varepsilon_{\mathbf{k}}, \tag{2.4}$$

where $\varepsilon_{\mathbf{k}}$ is the bare band energy of particle with quasimomentum $\hbar\mathbf{k}$. The function $\Phi(\eta)$ can be determined from the Taylor expansion; i.e.,

$$\Phi(\eta) = f_0 + f_1\eta + f_2\eta^2, \tag{2.5}$$

because with growing U, $\eta \to 0$. The coefficients f_0, f_1, and f_2 are found by imposing the following conditions:

(i) for $U = 0$ random site occupancy must prevail, whence $\eta = \langle n_{i\uparrow}\rangle \langle n_{i\downarrow}\rangle = n^2/4$;

(ii) The band energy for $U = 0$ must be equal to $\bar{\varepsilon}$, i.e., $\Phi(\eta = n^2/4) = 1$; and

(iii) The band energy in the limit $\eta = 0$ is

$$\Phi(\eta = 0)\bar{\varepsilon} = -(W/2)n(1 - n), \tag{2.6}$$

where W is the bare bandwidth of the band. These three conditions when imposed on Eq. (2.3), together with the equilibrium constraint $\partial E/\partial\eta = 0$, lead to the following relations:

$$f_0 = (1 - n)/(1 - n/2), \tag{2.7a}$$

$$f_1 = 4/[n(1 - n/2)], \tag{2.7b}$$

$$f_2 = -8/[n^3(1 - n/2)]. \tag{2.7c}$$

The optimal value of $\eta = \eta_0$ is then specified by

$$\eta_0 = \frac{n^2}{4}\left(1 - \frac{U}{U_c}\right), \tag{2.8}$$

with $U_c = 8|\bar{\varepsilon}| = 2W$ being the critical value of the parameter U above which there are no double occupancies. The value $U_c = 2W$ specifies the case with featureless form of the bare density of states (see below).

A special case of interest arises when there is exactly one electron per atom, i.e., when $n = 1$. In this special but important situation one finds from (2.8) and (2.5) and (2.7) that (*8, 10*)

$$\eta_0 = \tfrac{1}{4}(1 - U/U_c), \tag{2.9a}$$

$$\Phi(\eta_0) = 1 - (U/U_c)^2, \tag{2.9b}$$

$$E/N = \left(1 - \frac{U}{U_c}\right)^2 \bar{\varepsilon}. \tag{2.9c}$$

The quantity $\Phi(\eta_0)$ plays a role of an optimized band narrowing factor; for in the absence of electron correlations ($U = 0$) $\Phi(\eta_0) = 1$. Also, for $n = 1$ the band energy vanishes when $U = U_c$, i.e., when $\Phi(\eta_0) = 0$. To see directly that the nature of the ground state changes at $U = U_c$ we can calculate the magnitude of the square of the electron spin $\langle \mathbf{S}_i^2\rangle$, where the spin operator is defined through the relation

$$\mathbf{S}_i \equiv (S_i^{+}, S_i^{-}, S_i^{z}) = (a_{i\uparrow}^{+} a_{i\downarrow}, a_{i\downarrow}^{+} a_{i\uparrow}, (n_{i\uparrow} - n_{i\downarrow})/2). \tag{2.10}$$

One finds that

$$\langle \mathbf{S}_i^2\rangle = (\tfrac{3}{4})(1 - 2\eta_0). \tag{2.11}$$

For $U \to \mathbf{U}_c$, $\langle \mathbf{S}_i^2\rangle \to \frac{1}{2}(\frac{1}{2} + 1)$, i.e., one obtains an atomic value of the electron spin. This means that the singlet configurations on each atom have been suppressed and the spin and charge fluctuations are energetically separated. In other words, the elec-

trons cannot move from their atomic locations but their spins can fluctuate and correlate with those of electrons in neighboring localized states. The parameter η_0 plays a role of the order parameter for the correlated metal → magnetic insulator transition as we will see below.

One should note that the approach can be generalized to the magnetically polarized state, e.g., when the external magnetic field is applied. In these circumstances the band narrowing is spin dependent, i.e., $\Phi(\eta) \to \Phi_\sigma(\eta)$, with

$$\Phi_\sigma(\eta) = f_{0\sigma} + f_{1\sigma}\,\eta + f_{2\sigma}\eta^2. \tag{2.12}$$

A straightforward application of the conditions (i)–(iii) in this case yields (*11*)

$$f_{0\sigma} = (1 - \mathrm{n})/(1 - n_\sigma), \tag{2.13a}$$

$$f_{1\sigma} = 2/[n_\sigma(1 - n_\sigma)], \tag{2.13b}$$

$$f_{2\sigma} = 1/[n_\sigma^2 n_{-\sigma}(1 - n_\sigma)], \tag{2.13c}$$

so that

$$\Phi_\sigma = \frac{1}{1 - n_\sigma} \times [1 - n + (2/n_\sigma)\eta - (1/n_\sigma^2 n_{-\sigma})\eta^2]. \tag{2.14}$$

Note that Eqs. (2.13a–2.13c) and (2.14) reduce respectively to (2.7a–2.7c) and (2.5) for the unpolarized state, i.e., for $n_\sigma = n_{-\sigma} = n/2$.

Summarizing this section we emphasize that our approach is single-site in nature. This is because only the intraatomic correlations are treated properly while the intersite correlations are expressed via products of single-site probabilities (cf., expression (2.6) for the band energy for $\eta_0 = 0$ case). The system of $N_e = N$ electrons transforms into the system of localized magnetic moments for the critical value $U = U_c$ of intraatomic interaction. The metallic state of electrons for $U \to U_c$ (but below U_c) is called *the almost localized Fermi liquid*. The physical properties of this state will be discussed next, after the quasiparticle states representing almost localized electrons are defined.

3. Quasiparticle States and Properties of Almost Localized Electrons at $T = 0$

The normalized band energy can be calculated by defining the quasiparticle states with energy

$$E_{\mathbf{k}} = \Phi(\eta)\varepsilon_{\mathbf{k}}. \tag{3.1}$$

Namely, for these quasiparticle states obeying Fermi–Dirac statistics the distribution $f_{\mathbf{k}\sigma}$ for the band energy is

$$E_B/N = \sum_{\mathbf{k}\sigma} E_{\mathbf{k}} f_{\mathbf{k}\sigma}, \tag{3.2}$$

where

$$f_{\mathbf{k}\sigma} = \frac{1}{1 + \exp[\beta(E_{\mathbf{k}} - \mu)]}, \tag{3.3}$$

$\beta = (k_B T)^{-1}$ is the inverse temperature in energy units, and μ is the chemical potential. We can calculate (3.2) explicitly by determining the chemical potential from the equation

$$n = (1/N)\sum_{\mathbf{k}\sigma} f_{\mathbf{k}\sigma}. \tag{3.4}$$

For $T = 0$ and for a featureless form of the density of states (DOS), i.e., for

$$\rho(\varepsilon) = \begin{cases} 1/W & \text{for } -W/2 \le \varepsilon \le W/2 \\ 0 & \text{otherwise,} \end{cases} \tag{3.5}$$

we obtain $\mu = (n - 1)W/2$, and

$$E_B/N = \Phi(\eta)\bar{\varepsilon} = -\Phi(\eta)W(1 - n/2)n/2. \tag{3.6}$$

The physical interpretation of the fermion quasiparticles introduced above is as follows. We consider particle dynamics close to the Fermi surface, i.e., within the energy range $\pm k_B T$ centered on μ for given number $N_D = N\eta$ of double occupancies. The value at η is determined by the balance of much

larger energies $\bar{\varepsilon} < 0$ and $U > 0$. In other words, the quasiparticles are regarded as fermions with self-consistently adjusted bandwidth. The principal difference with respect to the Landau theory of the Fermi liquid is in the manner in which the interaction part is included. Here it is determined by variational calculations. Note that the quasiparticle energy (3.1) contains two-particle correlation function η which is determined variationally. The term "*correlated electrons*" bears its origin from incorporation of this type of correlation into the single-particle picture of electron states.

The quasiparticle interpretation presented above is supported by the explicit calculations of the average $\bar{n}_{\mathbf{k}\sigma}$ within the Gutzwiller approach (*12*). Namely, according to the Gutzwiller scheme,

$$\bar{n}_{\mathbf{k}\sigma} = (1 - q_\sigma)\bar{n}_\sigma + q_\sigma f_{\mathbf{k}\sigma}, \qquad (3.7)$$

where

$$q_\sigma = \frac{n_\sigma - \eta}{n_\sigma(1 - n_\sigma)} \left\{(1 - n + \eta)^{1/2} + \left[\frac{\eta(n_{-\sigma} - \eta)}{n_\sigma - \eta}\right]^{1/2}\right\}^2, \qquad (3.8a)$$

and $n_\sigma \equiv \langle n_{i\sigma}\rangle$. It is easy to show that the expression for q_σ coincides with that for Φ_σ given above for the case $n_\sigma = n_{-\sigma} = n/2$ and $n = 1$. On the other hand, q_σ is the discontinuity in the spin σ particle distribution at the Fermi surface. This means (*8*) that the effective mass renormalization (with respect to the bare band mass m_B) is

$$\frac{m_\sigma^*}{m_B} = q_\sigma^{-1}. \qquad (3.8b)$$

Note that in general (i.e., for $n < 1$) the effective mass is spin dependent; this is not so for $n = 1$, as can be seen from (3.8) by imposing the condition $n_\sigma + n_{-\sigma} = 1$. The case corresponding to the half-filled band state will be considered in detail below.

The mass enhancement factor q_σ^{-1} is **k**-independent. This is the reason why we can identify it with the inverse band narrowing factor (Φ^{-1}) which is determined from the global energy analysis. Taking $\Phi(\eta_0)$ in the optimized form (2.9b) one finds at $T = 0$

$$\frac{m_B}{m^*} = 1 - \left(\frac{U}{U_c}\right)^2, \qquad (3.9)$$

i.e., the quasiparticle mass is divergent as $U \to U_c$. The transformation of the metallic state into a system of localized moments at $U = U_c$ therefore represents a localization caused by the many-body interaction. The metallicity requires formation of ionic configuration M^+ and M^- out of the atomic M_0 states, and the M^- state involves energy U associated with the Coulomb repulsion which suppresses the formation of ionic states $M^\pm$ if $U > U_c$.

To show that the transition with $\eta_0 \to 0$ (i.e., $U \to U_c$) represents for $n = 1$ a true phase transition one can calculate (*8*) the magnetic susceptibility of the interacting metallic electrons in this case. This quantity is obtained by expanding q_σ to order m^2, where $m = \langle n_{i\uparrow} - n_{i\downarrow}\rangle$. We have then for $n = 1$

$$q_\sigma = q_m = 8\eta(1 - 2\eta) \times \left\{1 + \frac{m^2}{4}\left[4 - \frac{1}{(1 - 2\eta)^2}\right]\right\}. \qquad (3.10)$$

The corresponding ground state energy of the weakly magnetized state is then

$$E_G/N = q_m\bar{\varepsilon} + U\eta + \frac{m^2}{4\chi_0}q_m, \qquad (3.11)$$

where the last term expresses work performed on the system to magnetize it and χ_0 is the bare band Pauli susceptibility per site ($\chi_0 = 2\mu_B^2\rho^0(\varepsilon_F)$, where $\rho^0(\varepsilon_F)$ is the density of bare states per spin per site at the bare Fermi energy ε_F). Note that in deriving the last term in (3.11) we have taken the density

$\rho(\mu)$ of quasiparticle states (per spin per site) to be related to the corresponding quantity for the bare electrons via the relation

$$\rho(\mu) = \frac{\rho^0(\varepsilon_F = \mu/q_m)}{q_m},$$

which follows in a straightforward manner from (3.8). Substituting (3.11) and grouping the terms containing m^2 together and subsequently minimizing the resultant expression with respect to η one obtains

$$E_G/N = \bar{\varepsilon}\left(1 - \frac{U}{U_c}\right)^2 + \frac{m^2}{4\chi_0}\left(1 - \frac{U}{U_c}\right)^2 \times \left\{1 - U\rho^0(\varepsilon_F)\frac{1 + U/(2U_c)}{(1 + U/U_c)^2}\right\}. \quad (3.12)$$

On casting the whole second term into the form $m^2/4\chi$, we obtain an explicit form of the zero-field susceptibility for the interacting system in the form

$$\chi = \frac{\chi^0}{\left(1 - \left(\frac{U}{U_c}\right)^2\right)\left\{1 - U\rho^0(\varepsilon_F)\frac{1 + U/(2U_c)}{(1 + U/U_c)^2}\right\}}. \quad (3.13)$$

Thus, χ diverges at $T = 0$ either when (i) Φ_0 vanishes, i.e., when $U = U_c$, or when (ii)

$$\tilde{S} \equiv 1 - \rho^0 U \frac{1 + U/(2U_c)}{(1 + U/U_c)^2} = 0, \quad (3.14)$$

i.e., when the renormalized Stoner criterion is met. In case (i) the Mott (or Mott–Hubbard) transition to the insulating state takes place, whereas in the case (ii) shows that the system undergoes a phase transition to a ferromagnetic state. The divergence of χ establishes that a true phase transition has taken place in either case. For the rectangular DOS specified by (3.5) the normalized Stoner factor at the Mott transition is $\tilde{S} = \tilde{S}_0 = \frac{1}{4}$; i.e., no ferromagnetic instability can take place though χ is enhanced by the factor $(\Phi_0\tilde{S})^{-1}$ in the vicinity of the transition.

The expressions for the effective mass enhancement and χ permit an examination of the Fermi liquid characteristics of almost localized electrons. Namely, as will be shown explictly in the next section, the linear-specific heat coefficient γ is given by

$$\gamma = (m^*/m_B)\,\gamma_0, \quad (3.15)$$

where γ_0 is the linear coefficient for bare (band) electrons, i.e. has the form

$$\gamma_0 = \frac{2\pi^2}{3} k_B^2 \rho^0. \quad (3.16)$$

Also, the expression (3.13) for χ can be rewritten as

$$\chi = \left(\frac{m^*}{m_B}\right)\frac{\chi_0}{\tilde{S}}. \quad (3.17)$$

Therefore, the Wilson ratio R is

$$R \equiv \frac{\chi}{\gamma} \equiv \frac{\chi_0}{\gamma_0}\frac{1}{\tilde{S}}. \quad (3.18)$$

This ratio is finite at the metal to Mott insulator transition if $\tilde{S}$ is finite. This property of almost localized electrons distinguishes them from electrons for almost magnetic systems for which spin fluctuations greatly enhance χ and drive the magnetic transition for $U\rho^0 \to 1$. In the present description the Stoner factor $U\rho^0$ is reduced (cf., (3.14)) by the charge fluctuations which freeze out at the Mott ($U = U_c$) transition, i.e., for $\eta_0 = 0$.

One can draw the analogy between the present and the Landau theory of the Fermi liquid even further. Namely, starting from the standard parametrization of the interaction between the quasiparticles in the Landau theory (*13*) one obtains the following expression for the quantities of interest:

$$\gamma = \gamma_0(1 + \tfrac{1}{3}F_1^S) = \gamma_0(m^*/m_B) \quad (3.19)$$
$$\chi = \chi_0 \frac{m^*}{m_B}(1 + F_0^a)^{-1},$$

as well as for the bulk compressibility κ defined through

$$\frac{1}{\kappa} \equiv -V\frac{dp}{dV} = \rho^2 V \frac{\partial\mu}{\partial N_e}, \quad (3.20)$$

in the form

$$\kappa = \kappa_0(1 + F_0^S)^{-1}\frac{m^*}{m_B} \qquad (3.21)$$

In these equations F_0^a, F_0^S, and F_1^S are the standard interaction parameters, $\rho = N_e/V$ is the particle density within the volume V, and κ_0 is the compressibility for the bare electrons. Additionally, in deriving the second part of the relation (3.19), Galilean invariance has been assumed. To apply this invariance to the interacting electrons their momentum must be a good quantum number, i.e., one must be able to ignore the effect of the periodicity of the lattice which produces the interacting gas confinement within the volume V.

Using (3.9), (3.13) and the expression for $(\partial\eta/\partial N_e)$ derived by Rice and Brinkman in Ref. (*8*), one obtains the following explicit expressions for the parameters (*14*)

$$F_1^S = 3\{[1 - (U/U_c)^2]^{-1} - 1\}, \qquad (3.22)$$

$$F_0^a = -\rho^0 U\frac{1 + U/(2U_c)}{(1 + U/U_c)^2}, \qquad (3.23)$$

$$F_0^S = U\rho^0\frac{1}{1 + U/(2U_c)}\frac{1}{(1 - U/U_c)^2}. \qquad (3.24)$$

Note that ρ^0 describes the DOS for one spin direction only. The facts that close to localization $F_0^a \approx -\frac{3}{4}$ while κ drops precipitously and γ rises sharply have been used to characterize liquid ^{3}He as an example of an almost localized Fermi liquid. In other words, the solidification of liquid ^{3}He under pressure is regarded as an example of Mott localization, the localized moments being displayed by the nuclear spins of ^{3}He. We will return to this interpretation later, when discussing the localization process at nonzero temperature.

Finally, we discuss briefly properties of almost localized electrons in an external magnetic field (*11*). We have mentioned above (cf., Eq. (3.8)) that for $n < 1$ the effective mass is spin dependent. Figure 3 illustrates the spin direction dependence of the band narrowing factor in an applied magnetic field. The spin majority subband becomes wider with increasing magnetization while spin minority band narrows down. Equivalently, the effective mass for the majority subband $m_\uparrow^*$ is reduced to the band mass m_B when the magnetic polarization $m = \langle n_{i\uparrow} - n_{i\downarrow}\rangle \to 1$, while the corresponding mass in the spin minority subband grows spectacularly. The spin dependence of m^* is due to the circumstance that the correlation function $\eta \equiv \langle n_{i\uparrow} n_{i\downarrow}\rangle$ is reduced in the magnetized state and hence the Coulomb interaction part $U\eta$ is suppressed. The majority spin electrons encounter a small number of minority electrons and therefore in the $m_\uparrow^* \to 1$ limit they behave as band electrons ($\eta = 0$ then). By contrast, each of the minority electrons encounters many majority spin electrons and scatters strongly; hence, their mass is enhanced in the field (Fig. 4).

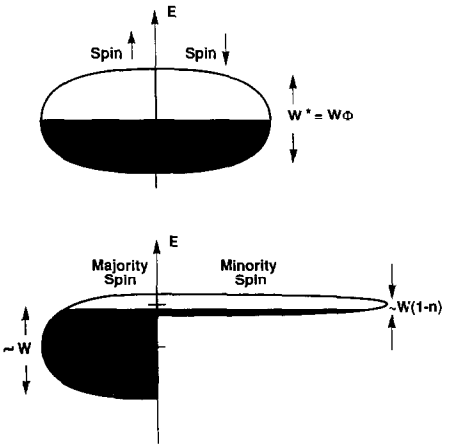

FIG. 3. Schematic representation of quasiparticle states in band narrowed by Coulomb repulsion both for the magnetic field $H_a = 0$ (top) and $H_a \neq 0$ (bottom).

Apart from the spin asymmetry there is an enhanced value of the spin splitting between the spin subbands. This enhancement leads to a strong field dependence of magnetization which thereby saturates in physically accessible fields. To demonstrate this prop-

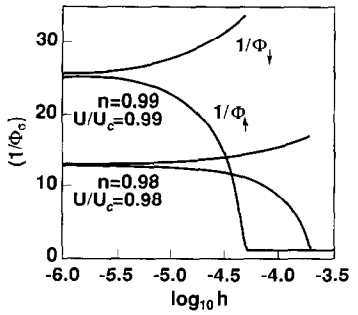

FIG. 4. The effective mass enhancement due to electron–electron interaction as a function of reduced field $h \equiv (\frac{1}{2})g\mu_B H/W$. The spin asymmetry of the enhancement is discussed in the text.

erty explicitly we calculate the magnetization curve for a DOS in the form (3.5) using the quasiparticle energies

$$E_{k\sigma} = \Phi_\sigma(\eta)\varepsilon_k - g\mu_B H_a \sigma/2, \quad (3.25)$$

where H_a is the applied magnetic field, g is the Landé factor, and μ_B is the Bohr magneton. The self-consistent equation for $n_\sigma = \langle n_{i\sigma}\rangle$ has the form

$$n_\sigma = \frac{1}{W\Phi_\sigma}\left\{\mu + \frac{W}{2}\Phi + g\mu_B H_a \sigma/2\right\}. \quad (3.26)$$

Taking Φ_σ as given by Eq. (2.14), the minimization of the groundstate energy with respect to η for $n \to 1$ leads to the relation

$$\eta_0 = \frac{n^2 - m^2}{4}\left\{1 - \frac{U}{U_c} \frac{(n^2 - m^2)[(1 - n/2)^2 - m^2/4]}{[n(1 - n/2) - m^2/2]^2 - m^2(1 - n)^2}\right\} \approx \frac{1 - m^2}{4}\left(1 - \frac{U}{U_c}\right\}. \quad (3.27)$$

Additionally, the magnetization curve is linear, i.e.,

$$m = \frac{g\mu_B H_a}{W} \frac{1}{(1 - U/U_c)^2}. \quad (3.28)$$

The presence of the factor $(1 - U/U_c)^{-2}$ makes possible the magnetization saturation in physically accessible fields and for U close to U_c. This property distinguishes almost localized electrons from quasiparticles forming an ordinary Fermi liquid. Conversely, the strong polarization arising from the applied field makes almost localized electrons to resemble localized moments into which they transform at $U = U_c$.

For $n = 1$ neither the band narrowing factor (2.14) nor the factor (3.8) depends on σ. Nevertheless, the effective mass varies strongly with magnetic field, as shown in Fig. 5. The magnetization curve in the half-filled band case is strongly nonlinear, as is demonstrated in Fig. 6. The strongly upward sweep in the $m(H)$ curve is regarded as a signature of almost metamagnetic behavior, as discussed in relation to ^{3}He in Ref. (*15*). The field dependence of η for this case is shown in Fig. 7. The singlet configuration of atoms is indeed suppressed with the growing field $h \equiv (1/2)g\mu_B H_a/W$.

In summary, in this section we have

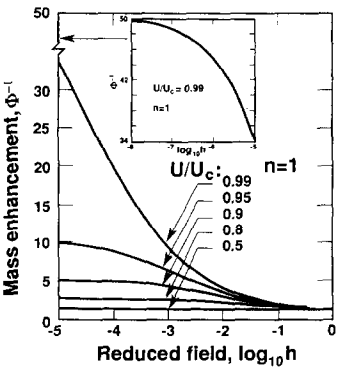

FIG. 5. Same as in the legend to Fig. 4 for $n = 1$ and U/U_c specified. Note the absence of the spin direction dependence of the mass enhancement for the half-filled band case.

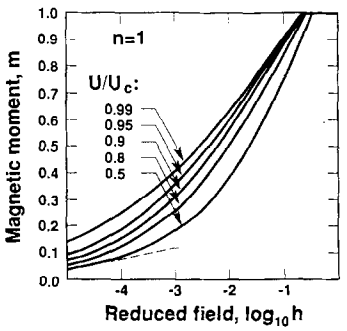

FIG. 6. Magnetic field dependence of the magnetic moment $m = \langle n_{i\uparrow} - n_{i\downarrow} \rangle$ per site. The magnetization curve is strongly nonlinear and saturates in physically accessible fields.

shown that the magnetic susceptibility and the effective mass are strongly enhanced close to the Mott transition because of the suppression of the charge fluctuations in the system. The mass is strongly enhanced for $U \to U_c$ because the charge transport throughout the system is impeded to the degree that η_0 diminishes. This mass enhancement corresponds to an enhancement of the DOS at the Fermi level by a factor $[1 - (U/U_c)^2]^{-1}$ by which the Pauli susceptibility is also correspondingly increased. The additional increase in χ arrives from the growth of the magnetic moment $\langle \mathbf{S}_i^2 \rangle$ with U. The magnetization of an almost localized Fermi liquid saturates in physically accessible fields; this is one of the precursory localization effects for $U \to U_c$.

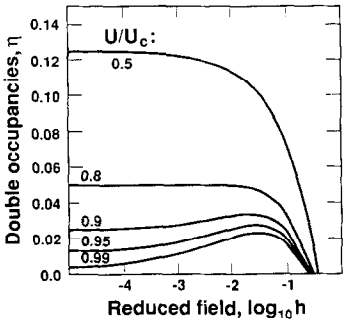

FIG. 7. Field dependence of the double occupancy probability η. The dependence is not monotonic for an almost localized Fermi liquid.

4. Low Temperature Properties of an Almost Localized Fermi Liquid

In this section we discuss the properties of an almost localized Fermi liquid in the low temperature regime. For this purpose we generalize the Sommerfeld expansion (*16*) developed originally for the description of an electron gas and extended later (*13*) to the case of interacting electrons.

We start from the expression for the normalized band energy at $T > 0$:

$$E_B/N = (1/N) \sum_{k\sigma} E_{k\sigma} f_{k\sigma} + U\eta. \quad (4.1)$$

From our interpretation of Φ_σ as a band narrowing factor, one can express the density $\rho^\sigma(E)$ of quasiparticle states (for one spin direction) via the corresponding quantity $\rho^0(\varepsilon)$ for the bare electrons. One finds (*9*) that

$$\rho^0(E) = \frac{1}{\Phi_\sigma} \rho^0 \left(\varepsilon \equiv \frac{E}{\Phi_\sigma} \right).$$

In the limit $n = 1$ of interest to us in this section we set $\Phi_\sigma \equiv \Phi$; therefore, the expression (4.1) can be rewritten in the following integral form

$$E_B/N = 2\Phi \int_{-W/2}^{W/2} d\varepsilon . \varepsilon . \rho^0(\varepsilon) . f\left(\frac{\varepsilon - \mu_0}{k_B T^*} \right), \quad (4.2)$$

where $T^* \equiv T/\Phi$ plays the role of effective temperature for the bare electrons, μ_0 is the chemical potential for the bare electrons, and the $(-W/2, W/2)$ energy interval determines the bare band limits. For the symmetric shape of the DOS assumed for the sake of simplicity, i.e., for $\rho(\varepsilon) = \rho(-\varepsilon)$, we find that $\mu \equiv 0$ for arbitrary T and H_a.

Analogously, we define the free energy functional per site as

$$\frac{F}{N} = \sum_{\mathbf{k}\sigma} E_{\mathbf{k}\sigma} f_{\mathbf{k}\sigma} + U\eta + \frac{k_B T}{N} \sum_{\mathbf{k}\sigma} \times [f_{\mathbf{k}\sigma} \ln f_{\mathbf{k}\sigma} + (1 - f_{\mathbf{k}\sigma}) \ln(1 - f_{\mathbf{k}\sigma})]. \quad (4.4)$$

This functional must be minimized with respect to η and m (in the magnetized state). For $n = 1$, $\Phi_\sigma = \Phi$ and Eq. (4.4) can be rewritten in the form

$$\frac{F}{N} = \Phi \frac{F_0(T^*, H^*)}{N} + U\eta, \quad (4.5)$$

where $H^* = H_a/\Phi$, and F_0 is the free energy for electron gas at temperature T^* and in the applied field H^*. This expression for F is related to the same quantity (F_0) for the bare electrons in the same manner as the total energy E is related to $\bar{\varepsilon}$ (cf., Eq. (2.3)). In other words, the bare states are in one-to-one correspondence to the interacting states both at $T = 0$ and for $T > 0$. Parameters such as the mass enhancement (Φ^{-1}) or the effective Zeeman splitting ($\mu_B H^*$) will depend on temperature.

Expression (4.5) permits a Sommerfeld-type expansion to be carried out on F_0 since this expression represents the standard formulation for the free energy of an electron gas. The detailed steps for a fourth-order expansion are very tedious (cf. the second Ref. (*10*)) and lead to the result

$$\frac{F}{N} = \Phi\bar{\varepsilon} + U\eta - \frac{\gamma_0 T^2}{2\Phi} - \frac{\pi^4}{36} \frac{(k_B T)^4}{\Phi^3} \left[\frac{7}{5}\rho - \frac{(\rho')^2}{\rho}\right] + \frac{m^2}{4\rho^0 \alpha(T^*)} + \ldots, \quad (4.6)$$

where

$$\alpha(T^*) \equiv | - \frac{\pi^2}{6}\left(\frac{k_B T}{\Phi}\right)^2 \left[\left(\frac{\rho'}{\rho^0}\right)^2 - \frac{\rho''}{\rho}\right] \quad (4.7)$$

and where ρ^0, ρ', and ρ'' are the bare density of states and its first and second derivatives, all taken at the bare Fermi level position ε_F. Eq. (4.6) must be still minimized with respect to η and m. This feature constitutes a principal difference between ordinary Sommerfeld expansion and the low T analysis for almost localized electrons. On minimizing (4.6) with respect to η one can determine several physical quantities of interest. Namely,

(i) the effective mass enhancement of quasiparticles for $H_a = 0$,

$$\frac{m^*}{m_B} = \frac{1}{1 - I^2}\left\{1 + \frac{2\pi^2 I^2}{3} \frac{(k_B T)^2 \rho^0}{|\bar{\varepsilon}|(1 - I^2)^3}\right\}, \quad (4.8)$$

where $I = U/U_c$. The particles become heavy for $I \to 1$; also as the equation shows, the mass m^* grows with T, signalling a percursory localization of almost localized electrons.

(ii) The zero-field-specific heat is found from $\partial E/\partial T$ as

$$C_V = \frac{\gamma_0 T}{\Phi_0} + \frac{3\gamma_0^2 T^3}{|\bar{\varepsilon}|\Phi_0^4} I^2 + \frac{\pi^4}{3} \frac{k_B^4}{\Phi_0^3}\left[\frac{7}{5}\rho'' - \left(\frac{\rho'}{\rho}\right)^2\right] T^3, \quad (4.9)$$

where $\gamma_0 = (2/3)\pi^2 k_B^2 \rho^0$ is the linear coefficient in the specific heat per site for bare (band) electrons. The presence of electron correlations manifests itself in the renormalization of $\gamma \sim (1 - I^2)^{-1}$, and in the *positive* T^3 term. It has been shown recently (*17*) that an inclusion of nonlocal spin fluctuation starting from the Gutzwiller state as a reference (mean-field) type of state leads to a $T^3 \ln(T/T_0)$ contribution to C_V instead of T^3 contribution provided in (4.9).

(iii) The zero-field susceptibility for $U \to U_c$ is found from $\partial^2 F/\partial H_a^2$ to yield

$$\chi \approx \frac{\chi_0}{1(1 - I)(1 - 3\rho U_c/8)}\left[1 - \bar{d} \frac{\pi^2 (k_B T)^2 \rho^0}{2U_c(1 - I)(1 - 3U_c/8)}\right] \quad (4.10)$$

where

$$\bar{d} \equiv \frac{U_c}{12\rho(1 - I)}\left[\left(\frac{\rho'}{\rho}\right)^2 - \frac{\rho''}{\rho}\right] - \frac{3}{(1 - I)^2}$$

$$\times \left(1 - \frac{1}{6}\rho U_c\right), \qquad (4.11)$$

and $\chi_0 = 2\mu_B^2\rho_0$ is the Pauli susceptibility (per site) for the bare electrons. We see that the T^2 term is strongly enhanced for $I \to 1$.

Summarizing, the low T properties of almost localized systems are similar to those for almost magnetic system (*18*). The quasiparticle picture presented above thus corresponds to a paramagnetic heavy electron metal with enhanced spin fluctuations. These fluctuations may lead to a superfluid state as is the case for liquid ^{3}He (*14*); the corresponding superconducting state with pairing mediated by an exchange of the spin fluctuation among almost localized charged fermion is not yet found, although both heavy fermion systems and high T_c superconductors seem to be strong candidates.

We have mentioned above that the Mott–Hubbard localization for $T = 0$ may be regarded as a continuous phase transition; the optimal double occupancy derived earlier, i.e.,

$$\eta_0 = \begin{cases} (1/4)(1 - U/U_c) & \text{for } U \le U_c \\ 0 & \text{for } U \ge U_c, \end{cases}$$

can be regarded as a mean-field order parameter describing the Mott–Hubbard localization: This electron localization reflects the change in character of χ from Pauli to Curie behavior; this change in turn is signaled by the divergent susceptibility as $U \to U_c$. In the next section we discuss in detail the nature of metal–insulator transition associated with this localization at nonzero temperature.

5. Discontinuous Metal–Insulator Transitions at $T > 0$

In this section we discuss a theory that deals with first-order metal–insulator at nonzero temperature. The boundary between the metallic state of almost localized electrons and the insulating state composed of localized magnetic moments is determined from the coexistence condition recurring that the free energies for these two states coincide. In other words, we treat the two states as separate phases in the thermodynamic sense. This approach leads to rationalization of both metal–insulator transitions and of the reentrant metallic behavior in the high temperature regime, observed in Cr-doped V_2O_3 systems (*18*). The experimental results for the system $(V_{1-x}Cr_x)_2O_3$ are shown in Fig. 8 where the temperature dependence of the resistivity is drawn (*19*). The family of the curves presented in that figure is the basis of the phase diagram plotted in Fig. 9. At

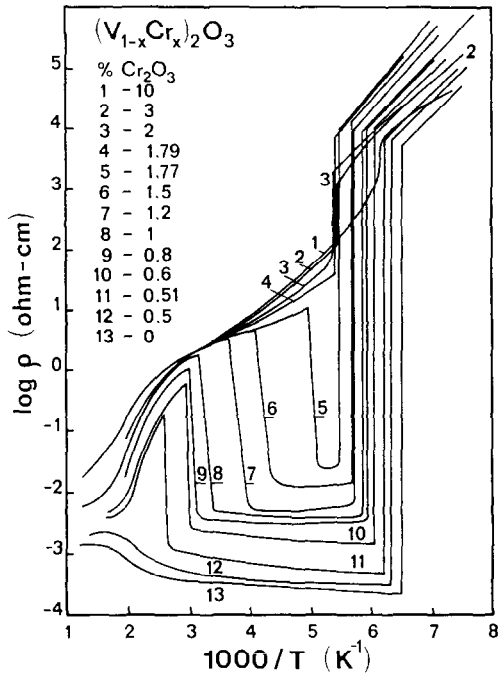

FIG. 8. Experimental measurements (*19*) of resistivity in the logarithmic scale as a function of inverse temperature $1000/T$ for the $(V_{1-x}Cr_x)_2O_3$ system. The atomic content x of Cr_2O_3 in V_2O_3 for each curve is specified.

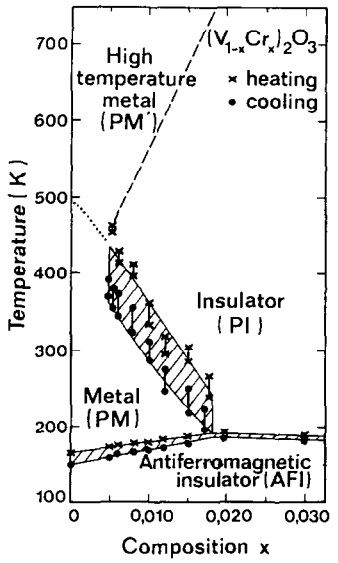

FIG. 9. The phase diagram of the $(V_{1-x}Cr_x)_2O_3$ system on the T–x plane. The continuous lines with hysteresis represent first-order boundaries between the phases specified.

low temperature the alloy is an antiferromagnetic insulator (AFI); in the vicinity of $T_{M'} = 170$ K a drastic change to a paramagnetic metal (PM) phase suddenly sets in; near $T_{MI} \approx 295$ K the material experiences in a narrow Cr concentration range to a paramagnetic insulator (PI), and on further heating the alloy gradually reverts back to a metallic state (PM') above 600 K, which is rather similar to the low temperature (PM) phase encountered for $170\ \text{K} \leq T \leq 295\ \text{K}$. The metallicity at intermediate and high temperatures, separated by a region of insulating properties, is termed *reentrant metallic behavior.*

The principal feature of Mott localization is associated with the fact that band and interaction parts in the total energy (2.3) almost compensate each other. Hence, the much smaller entropy or applied field contributions influence the stability of localized phase against the Fermi liquid state, as we will see in this Section.

5.1. Mott Localization of Almost Localized Electrons: Low Temperature Regime

The free energy functional (per site) for the correlated electron assembly is given in the lowest order by

$$\frac{F}{N} = \Phi\bar{\varepsilon} + U\eta - \frac{\gamma_0 T^2}{2\Phi}. \tag{5.1}$$

Minimization with respect to η leads to

$$\frac{F}{N} = (1-I)^2\bar{\varepsilon} - \frac{\gamma_0 T^2}{1-I^2}. \tag{5.2}$$

The Mott (or Mott–Hubbard) localization is a transformation of itinerant (almost localized) electrons in a half-filled band into a lattice of localized moments. The free energy of those moments which can randomly be in the spin-up or spin-down orientation may be expressed as

$$\frac{F_I}{N} = -k_B T \ln 2. \tag{5.3}$$

The coexistence condition determining the localization boundary is $F = F_M$, or, explicitly,

$$\frac{F}{N} = -k_B T \ln 2. \tag{5.4}$$

This condition yields two transition temperatures

$$k_B T_\pm \approx \frac{3\Phi_0}{2\pi^2\rho_0}\left\{\ln 2 \pm \left[(\ln 2)^2 - \frac{4}{3}\times \pi^2\rho_0|\bar{\varepsilon}|(1-I)^2/\Phi_0\right]^{1/2}\right\}. \tag{5.5}$$

For a DOS in the form (3.5) these temperatures are

$$\frac{k_B T_\pm}{W} = \frac{3}{2\pi^2}\left[1 - \left(\frac{U}{2W}\right)^2\right]\times \left\{(\ln 2)^2 \pm \left[(\ln 2)^2 - \frac{1-U/2W}{1+U/2W}\right]^{1/2}\right\}, \tag{5.6}$$

as represented by a retrograde curve in Fig. 10. The lower part of the curve corresponds to the T_- solution while the upper corresponds to T_+. The two solutions meet at critical point $U = U_{lc}$ given by

$$\frac{U_{lc}}{U_c} = 1 - \frac{\sqrt{3}\ln 2}{2\rho} \frac{1}{(\rho^0|\bar{\varepsilon}|)^{1/2}}. \quad (5.7)$$

The corresponding transition temperature $T = T_c$ is

$$k_B T_c = \frac{3\ln 2}{2\pi^2 \rho^0} \left[1 - \left(\frac{U_{lc}}{U_c}\right)^2\right]. \quad (5.8)$$

For $U \leq U_{lc}$ the Fermi liquid state is stable for all T.

From inspection of Fig. 8 it is clear that for $U/U_c > 1$ only the localized state is encountered. For U/U_c in the range $U'_{lc} < U < U_c$ there is a single paramagnetic metal (PM)—paramagnetic insulator (PI) phase transition. For $U_{lc} < U < U'_c$ two phase transition are found with raising temperature: this is the regime of reentrant metallic behavior, with the PM $\rightarrow$ PI $\rightarrow$ PM′ sequence as temperature is raised. Strictly speaking, the existence of the point at $U = U'_c$ can be proven only by recourse to a more general approach discussed in Section 5.2.

Reentrant metallic behavior is readily understood from a physical point of view. Namely, at temperatures close to $T = 0$ the entropy of disordered localized moments is large and equal to $k_B \ln 2$ per electron (we neglect any magnetic ordering effects for the time being), whereas in the Fermi liquid it grows linearly with T from zero. Hence at $T = T_-$ the free energy of localized particles outweighs that of the Fermi liquid, even though at $T = 0$ the opposite is true. However, as the temperature rises, the Fermi liquid entropy grows and approaches the value $2k_B \ln 2$ in the high T limit. Thus, the metallic phase must become stable again in the high temperature limit. The detailed shape of the phase boundary is determined by an interplay between the competing energy and entropy contributions. The competitive nature of the energetics associated with the two phases involved is shown schematically in Fig. 9, where the free energy of the metallic phase is represented by the parabolas while the straight line represents the phase with localized electrons. We show next that the above features are also encountered in a more general approach (*20*) which we discuss next.

5.2. Metal–Insulator Transitions at Arbitrary Temperature: Two-phase model

As emphasized earlier for $T = 0$ (cf., Section 2), the general formulation of localized vs itinerant electron state dichotomy is based on the idea that close to the Mott transition the band ($\bar{\varepsilon}$) and Coulomb (U) energies are of comparable magnitude. Therefore, both the atomic and band aspects of the electronic states should be treated on an equal footing. To express this equivalence within a workable scheme at arbitrary T we introduced the idea (*20*) that the band narrowing factor $\Phi(\eta)$ renormalizing the bare band energy $\bar{\varepsilon}$ in (2.3) describes the fraction of electrons of itinerant (extended) character, whereas $(1 - \Phi)$ represents the portion of the localized (atomic) character. This subdivision is also apparent in (3.7) where the average number n_σ of particles in the state $|k\sigma\rangle$ is composed of a fraction q_σ in the quasiparticle state and $(1 - q_\sigma)$ is composed of a fraction of particles in the atomic configuration $|i\sigma\rangle$. This subdivision had been introduced early on in the development of Gutzwiller approach (*21*). Such a subdivision follows also from the fact, introduced in Section 2 that $\Phi(\eta)$ is proportional to the conditional probability that a hopping process will take place in a correlated system. Accordingly, we will phenomenologically divide the entropy into two parts:

1. The fraction ΦN of the total number $N_e = N$ electrons with energies $E_k = \Phi\varepsilon_k$

contributes to the fermionic part, i.e.,

$$\frac{S_i}{N} = -\frac{\Phi}{N} k_B \sum_{k\sigma} [f_{k\sigma} \ln f_{k\sigma} + (1 - f_{k\sigma}) \ln(1 - f_{k\sigma})], \quad (5.9)$$

and

2. The fraction $(1 - \Phi)N$ provides a contribution to the localized-moment part, i.e.

$$\frac{S_L}{N} \equiv k_B (1 - \Phi) \sum_{i=1}^{4} p_i \ln p_i$$
$$= -(1 - \Phi) k_B [(1 - 2\eta) \ln(1 - 2\eta) - (1 - 2\eta) \ln 2 + 2\eta \ln \eta]. \quad (5.10)$$

The quantities $p_1 \ldots p_4$ represent the probabilities of empty site, single occupancy with spin up or down, and doubly occupied site configurations which are respectively η, $(1 - 2\eta)/2$,$(1 - 2\eta)/2$, and η. Within this model the total free energy functional is given by

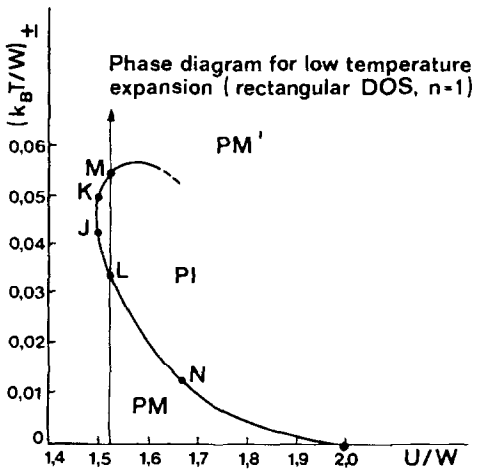

FIG. 10. Schematic representation of the phase diagram between paramagnetic metallic (PM and PM') and paramagnetic insulating (PI) phases. The vertical line indicates the sequence of phases encountered for a given system as a function of temperature. The points J to M correspond to the coexistence points of the two phases, as shown in the next Figure.

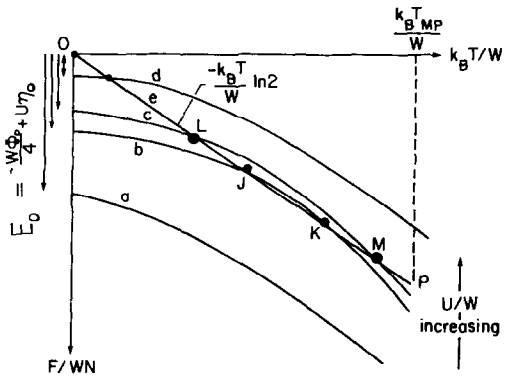

FIG. 11. Plots of temperature dependence of the free energies for the paramagnetic Mott insulator (the straight line starting from the origin) and the correlated metal (the parabolas a–d correspond to growing U/U_c ratio from $U < U_{lc}$ to $U_c' < U < U_c$). The points of crossing L and J correspond to a discontinuous PM → PI transition, while those at K and M correspond to the reverse (PI → PM') transition.

$$\frac{F}{N} = \Phi(\eta)\bar{\varepsilon} + U\eta - \frac{T(S_i + S_L)}{N}. \quad (5.11)$$

The minimization of (5.11) with respect to η and the subsequent calculations of the physical properties have been performed for a featureless (rectangular DOS (3.5) (*20*). In Fig. 12 we provide the metal–insulator boundary in the paramagnetic phase. The boundary line represents the first-order transition line excepting the three points that are marked explicitly. The diagram in Fig. 12 is similar to that shown in Fig. 8. However, the present two-phase model provides a justification for the simplified reasoning provided in the preceding section: In the PI phase Φ is negligibly small, whereas in the PM and PM' state Φ is appreciable. Hence the mixed phase approach provides a stable solution with either Fermi liquid or localized moment characteristics, as postulated earlier in the single-phase model.

As an example we have applied our theoretical calculations to the $(V_{1-x}Cr_x)_2O_3$ sys-

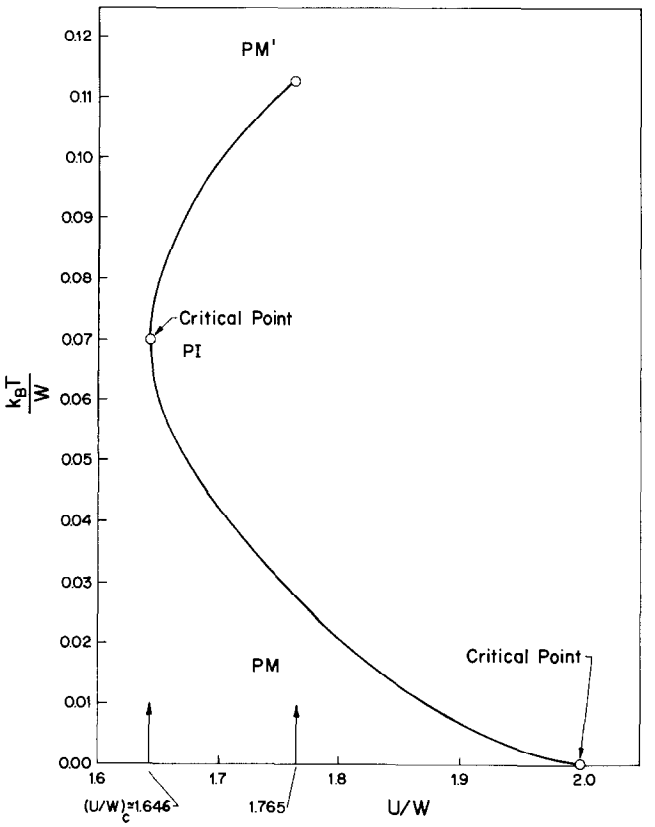

FIG. 12. Phase diagram in the paramagnetic region within a two-phase model discussed in the text.

tem; we plot in Fig. 13 the value of η on a logarithmic scale as a function of $1/T$. The inset shows the corresponding data of conductivity vs $1/T$ in the paramagnetic phase. The trends are similar, although the data do not exhibit the weak, high temperature discontinuity predicted by our theory. The absence of the high temperature discontinuity in the experiment may be attributed to the effect of lattice relaxation with changing carrier concentration in the high temperature regime. A quantitative theoretical analysis would require taking into account the electron–lattice interaction. One can also calculate explicitly the entropy of the transition; this quantity was discussed in Ref. (*20*).

Summarizing this section, we emphasize that within the present treatment the first-order metal–insulator boundary from the metallic side specifies the limit of applicability of the concept of the Fermi liquid (i.e., the liquid for which the Luttinger theorem (*22*) holds) and the limit below which the Fermi–Dirac distribution can be applied to describe the distribution of the quasiparticle states at nonzero temperature. Also, one should point out the principal difference between the Bloch–Wilson and Mott (magnetic) insulators. Namely, the Bloch–Wilson insulators (*16*) are diamagnetic since the filled band states are separated by a gap from empty (conduction) states. The Mott insulator corresponds to a half-filled band

configuration if electron correlations are not taken into account. It is a paramagnetic or an antiferromagnetic insulator. The existence of paramagnetic insulators with an odd number of electrons in $3d$ or $4f$ shells provides the most obvious example of the applicability of Mott–Hubbard concepts of localized electron states induced by electron–electron interactions.The canonical examples are MnO and CoO.

One should emphasize that the whole present analysis is based on Gutzwiller (single-site) approximation. It leads to the Mott–Hubbard localization only in the half-filled band case. The description of an insulating phase for $n < 1$, as observed in high T_c systems, requires inclusion of non-local trapping and disorder (*18*). Also, most of the theoretical approaches concentrated on calculating the transition point as a function of U/W; the present approach provides the discussion of the transitions along the temperature axis for fixed U/W.

6. Incorporation of Antiferromagnetic Ordering

In this section we examine the effect of antiferromagnetic ordering on the quasiparticle picture of almost localized electrons. As we have mentioned in the Introduction, the kinetic exchange interactions has been considered in the limit $U \gg W$. To generalize the applicability of this form of interaction to the regime close to the metal–insulator transition we introduce the factor $(1 - \Phi)$ representing the portion of the total number of electrons in the localized state. In effect, the exchange Hamiltonian has the form (*10*)

$$H_{ex} = \frac{4t^2}{U}(1 - \Phi)\sum_{\langle ij \rangle} \left\{ \mathbf{S}_i \cdot \mathbf{S}_j - \frac{1}{4}(1 - 2\eta_i)(1 - 1\eta_j) \right\}. \quad (6.1)$$

In this expression t is the transfer integral, the spin operator $\mathbf{S}_i$ is defined via (2.10), $\eta_i \equiv n_{i\uparrow} n_{i\downarrow}$, and $\langle ij \rangle$ limits the summation to the possible nearest neighbor pairs. This term should be added to the quasiparticle Hamiltonian considered before. Thus, the total Hamiltonian is given by

$$H = \Phi \sum_{\mathbf{k}\sigma} \varepsilon_{\mathbf{k}} n_{\mathbf{k}\sigma} + U\eta + H_{ex}. \quad (6.2)$$

The antiferromagnetically ordered lattice in the simplest situation is represented by two interpenetrating sublattices A and B such that each outer shell electron belonging to A has spin up and is surrounded by nearest neighbors belonging to B with spins down, and vice versa. The superstructure formed this way (a doubling of unit cell volume for some structures) leads in the mean-field approximation to a splitting of the narrow band into two *Slater subbands* with dispersion relations (*22*)

$$E_{\mathbf{k}1,2} = \pm[(\Phi\varepsilon_{\mathbf{k}})^2 + \Delta^2]^{1/2}, \quad (6.3)$$

where the Slater gap $2\bar{\Delta} \equiv Jz\langle S^z \rangle$, $J \equiv (4t^2/U)(1 - \Phi)$, and $\langle S_z \rangle = \langle n_{i\uparrow} - n_{i\downarrow} \rangle/2$ is the sublattice magnetization (the magnetic moment per site is $g\mu_B\langle S^z \rangle$). The Slater subbands are schematically represented in Fig. 14. The halving of the original band into two separate subbands, each containing N states, is caused by the magnetic superstructure. Therefore, the ground state of the antiferromagnetic system in the half-filled band case will be insulating. This insulating state represents a Slater insulator, with the bands narrowed by the electron correlations. As the Néel temperature is approached $\langle S^z \rangle \to 0$ and the two subbands merge into a single band. Therefore, the paramagnetic state of the Slater insulator is always metallic while that of a Mott insulator can be still insulating if the value of U is sufficiently large ($\sim U_c$).

The sublattice magnetization in this approach is calculated in a self-consistent way by minimizing the ground state energy with respect to $\langle S^z \rangle$. In the case of a featureless DOS (3.5) one can calculate this energy explicitly, yielding the result

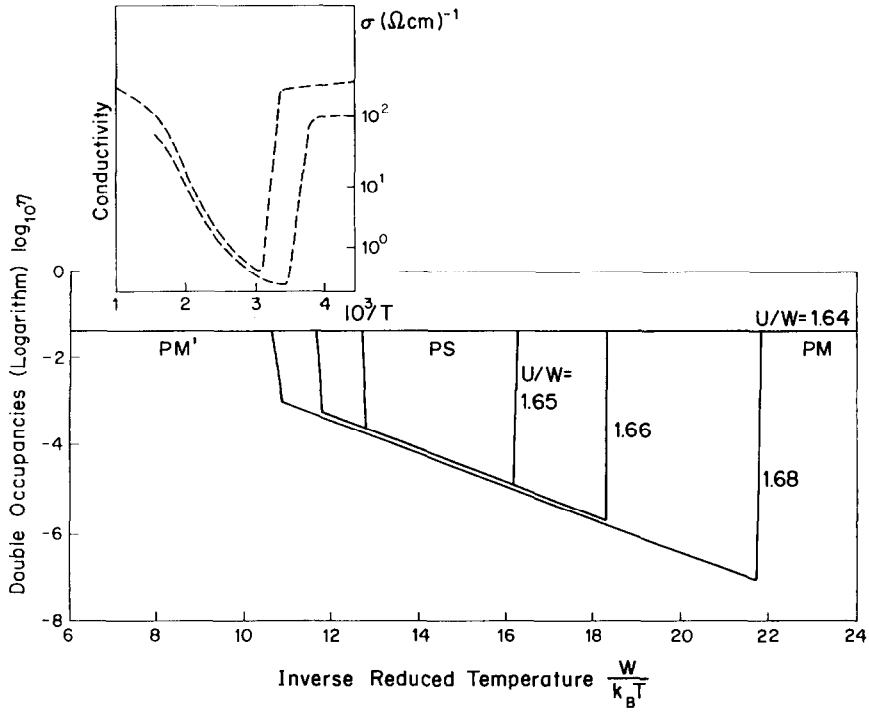

FIG. 13. The double occupancy η (in the logarithmic scale) as a function of inverse temperature W/k_BT for the two-phase model. The representative conductivity curve for $(V_{1-x}Cr_x)_2O_3$ system vs $10^3/T$ has been shown for comparison. The quantity η describes the carrier concentration for the system.

$$E_g/N = \frac{1}{2}\left[\left(\frac{\Phi W}{2}\right)^2 + \bar{\Delta}^2\right]^{1/2} - \frac{\bar{\Delta}^2}{W\Phi}\ln\left(\left\{\left[\left(\frac{W\Phi}{2}\right)^2 + \bar{\Delta}^2\right]^{1/2} + \frac{W\Phi}{2}\right\}/\bar{\Delta}\right) + U\eta - (Jz/8)(1-2\eta)^2 + 2\bar{\Delta}^2/Jz. \quad (6.4)$$

In the localized limit, where $\Phi \to 0$ we obtain

$$E_g/N = -Jz/4. \quad (6.5)$$

Thus, the ground state energy reduces to that of the Heisenberg antiferromagnet calculated in the molecular field approximation.

In order to be able to minimize Eq. (6.4) explicitly we need to know the band narrowing factor in the antiferromagnetic phase, i.e., the function $\Phi \equiv \Phi(\eta,m)$. This problem has been examined within the Gutzwiller approach in Ref. (*23*). For small magnetization one can take $\Phi(\eta, m) \approx \Phi(\eta)$, where $\Phi(\eta)$ is specified for the paramagnetic phase. Under this condition one obtains from (6.4) that

$$\langle S^z\rangle = \frac{(\Phi W/Jz)}{\sinh(2\Phi W/Jz)}. \quad (6.6)$$

As $\Phi \to 0$, $\langle S^z\rangle \to \frac{1}{2}$ as expected for a Heisenberg magnet in the strictly localized limit. The model DOS (3.5) for the bare electrons is simple enough to permit the calculation of the shape of Slater subbands. Namely, the density of quasiparticle states is

$$\rho^0(E) = \frac{2}{W\Phi}\frac{|E|}{(E^2 - \bar{\Delta}^2)^{1/2}}, \quad (6.7)$$

where $\bar{\Delta} \le |E| < -[(\Phi W/2)^2 + \bar{\Delta}^2]^{1/2}$. Note that the starting (rectangular) of bare DOS

is greatly altered in the AF phase. In the limit $\Phi \to 0$ the Slater subbands (narrowed by correlations) reduce to two discrete levels separated by energy $2\bar{\Delta}$ (Fig. 14). These levels are the spin split levels in the Heisenberg antiferromagnet. In other words, the Mott insulator represents a limiting case of Slater-type picture if band narrowing factor is included in the quasiparticle picture.

An important question for us is whether the itinerant (Slater-type antiferromagnet can transform discontinuously into a Mott insulator. Such calculations have been performed by Datta (*22*) taking the band narrowing for a paramagnetic phase. Within this approximation and for the featureless DOS we have to determine the character of the phase boundary between antiferromagnetic insulating and paramagnetic metallic phases. As we will argue in the next section, the AFI $\to$ PM transition takes place for temperatures well below the intrinsic Néel temperature T_N which for V_2O_3 is the 600 K regime. Therefore, when considering the free energy of AFI phase we adopt the low temperature approximation

$$F_{AF} = -Jz/8 + AT^4,$$

where the second term is the thermal contribution due to long wavelength acoustic magnon excitations, and A is related to the exchange stiffness constant. The first order AFI $\to$ PM transition temperature T_{MI} is determined by the coexistence condition $F_A F = F$, where F is given by Eq. (5.1). This condition yields

$$T_{MI} = \frac{1}{2A}\left\{\left[\left(\frac{\gamma_0}{\Phi_0}\right)^2 + 4A.\Delta E\right] - \frac{1}{2}\frac{\gamma_0}{\Phi_0}\right\}^{1/2}, \tag{6.8}$$

where

$$\Delta E = \bar{\varepsilon}\left(1 - \frac{U}{U_c}\right)^2 + Jz/8$$

is the difference between the groundstate energies in the metallic and insulating states. Positive values of T_{MI} occur only for $\Delta E > 0$, i.e., when the stable phase at $T = 0$ is antiferromagnetic. As $U \to U_c$, ΔE increases and so does T_{MI} as is experimentally observed (cf., Fig. 9).

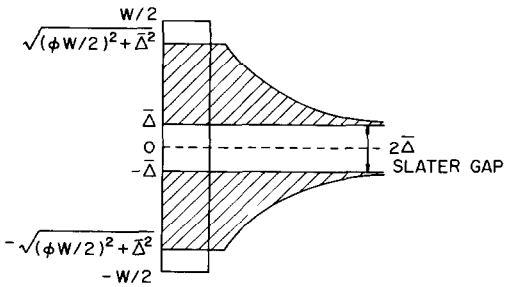

FIG. 14. The density of quasiparticle states showing the Slater splitting with the gap $2\bar{\Delta}$. The rectangular DOS is shown for comparison. Φ is the band narrowing factor.

7. Interpretation of Properties of V_2O_3 System

The metal-insulator transitions in pure and doped V_2O_3 involve not only discontinuous electronic transitions displayed in Fig. 8, but also accompanying magnetic (Fig. 15) and structural changes. In the present analysis we assume that the electron–electron interaction provide the principal driving force of these transitions; therefore we limit our discussion of the overall features observed (*18, 19*) to a purely electronic model. Namely, combining the results obtained in Section 5 and concerning the PM $\to$ PI $\to$ PM′ sequence of transitions with the discussion of AFI $\to$ PM transition in Section 6 we can draw the schematic phase diagram shown in Fig. 16. In this diagram we have also marked regimes correspondingly to different V_2O_3 alloy systems. Later we provide a discussion of the concepts developed above to those systems.

As mentioned in Section 5.1, three critical

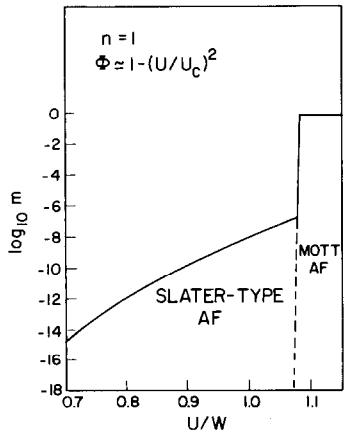

FIG. 15. Plot of the magnetic polarization m (in the logarithmic scale) vs U/W. The quantity m expresses the sublattice magnetic moment in the ground state.

values of U are important: U_{lc}, U_c', and U_c. The pure V_2O_3 system must be regarded as being characterized by a value of U near the vertical line $U = U_{lc}$, since with a small substitution of Cr for V the reentrant metallic behavior and PI phase are evident (cf., Figs. 8 and 9). One should note that the addition of Cr increases the U/W ratio; this is easily understood because the Cr_2O_3 system is a Mott insulator. Microscopically, Cr^{3+} is to the right of V^{3+} so the ion along the $3d$ transition metal series has a half-filled $3d$ set of levels. Hence, the extent of $3d$ wave function (and hence the value of bare bandwidth W) is smaller in the former case. The opposite is also true (*25*); namely that the substitution of Ti for V decreases the U/W ratio and eventually eliminates the antiferromagnetism with localized moments. The same effect is achieved by applying external pressure (*26*); the related experimental results for the $(V_{1-x}Ti_x)_2O_3$ system and for the pure V_2O_3 system under pressure are summarized in Fig. 17. The critical concentration for disappearance of AFI → PM transition is $x_c \approx 0.05$ while the corresponding critical pressure for the pure system is ≈25 kbar (*26*). As can be seen in Fig. 17 the linear specific heat close to the onset of insulating phase is strongly enhanced and the magnetic susceptibility is large and Pauli like (see the plots for $x = 0.051$). These results correlate very well with the theoretical discussion of properties of almost localized electrons in Section 4. Additionally, the large T^2 term in resistivity of the metallic phase for $T \to 0$ directly confirms the importance of electron–electron interactions.

The proposed phase diagram (Fig. 16) contains a boundary line between the two antiferromagnetic phases: Mott (AFI) and Slater (AFM) states. The antiferromagnetic metallic (AFM) phase with a small moment and low Néel temperature has been actually observed both in the $(V_{1-x}Ti_x)_2O_3$ system for $x \geq x_c$ as well as in the $V_{2(1-y)}O_3$ system (*27*). One should note that metallicity arises from the presence of holes in the lower Slater subband created by the *Ti* substitution for V, or by the presence of excess oxygen in $V_{2(1-y)}O_3$ case. The circumstance that these nonstoichiometric systems remain insulating for small deviation from

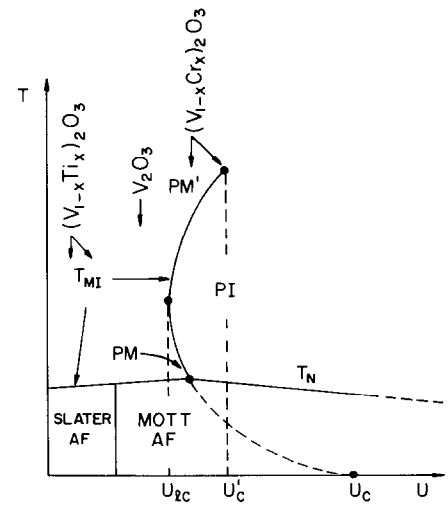

FIG. 16. Schematic phase diagram for the V_2O_3 system. The details are provided in the main text.

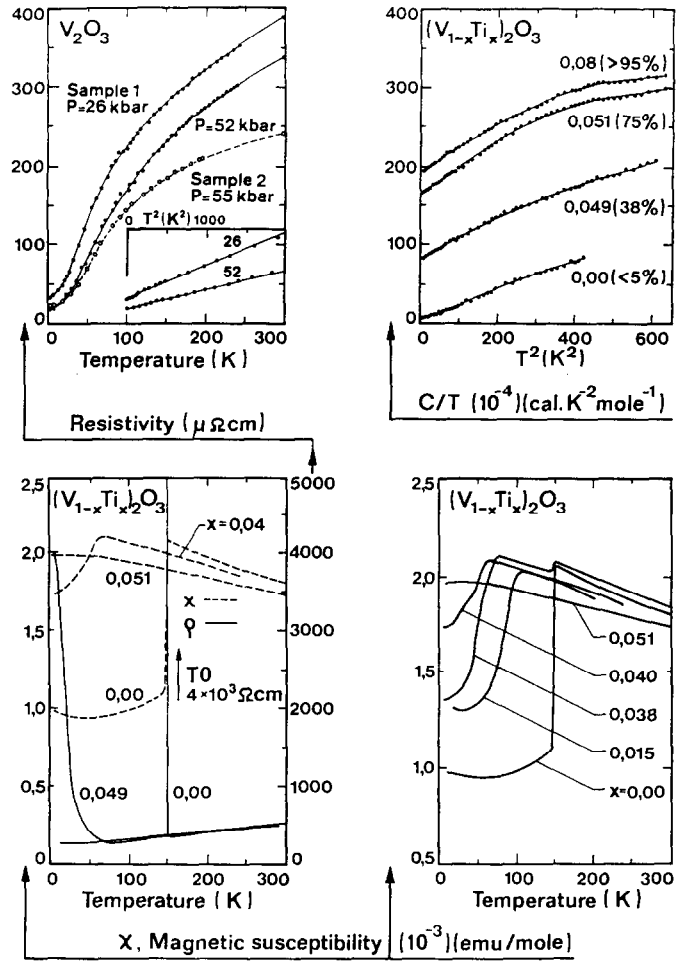

FIG. 17. The collected data for V_2O_3 under pressure (top left) and for $(V_{1-x}Ti_x)_2O_3$ systems as a function of temperature. For the details, see the main text.

ideal stoichiometry (e.g., for $0 < x < x_c$) provides an argument in favor of hole trapping in the Mott insulators. A similar behavior is observed in the $La_{2-x}Sr_xCuO_4$ system for $x \leq 0.05$ (*28*). Also, the role of disorder in localizing the holes should not be ignored.

One should note that the magnetic susceptibility in the localized moment (AFI) phase is smaller than in PM phase above the transition; it is also smaller than that in the paramagnetic phase of almost localized electrons. First, the magnitude of the local moment in both insulating and metallic phases does not change much since, as we have shown, $\langle \mathbf{S}_i^2 \rangle = \frac{3}{4}(1 - 2\eta) \approx \frac{3}{4}$. Therefore, the difference in χ must be ascribed to a different strength of the AF interaction in the two phases and to a large enhancement of χ in the metallic phase. The strength of interaction is reduced by factor $(1 - \Phi_0)$ in (6.1), which jumps in a discontinuous manner at the AFI $\rightarrow$ PM transition.

The PM phase stabilized by Ti addition (or excess oxygen) exhibits a universal be-

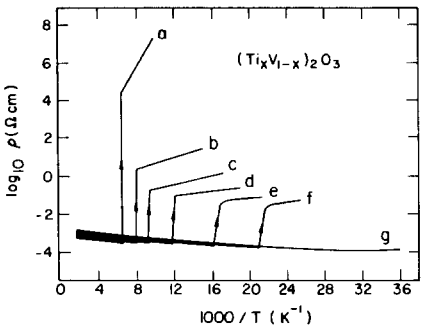

FIG. 18. Evolution of the AFI → PM transition temperature for $(V_{1-x}Ti_x)_2O_3$ system. The concentrations x are (*29*) *a*, 0.0; *b*, 0.01; *c*, 0.02; *d*, 0.03; *e*, 0.04; *f*, 0.049; and *g*, 0.055. Note the universal baseline common for all the samples.

havior illustrated by Fig. 18 (*29*). Namely, the temperature dependence of resistivity in the metallic phase is represented by the universal baseline, which is to a large extent independent of x. This x independence means that the disorder introduced by the Ti substitution plays only a secondary role in the metallic phase of $(V_{1-x}Ti_x)_2O_3$. This is not so in the insulating phase well below T_{MI}, where the electric transport is dominated by variable range hopping (*30*). Also, the metallic phase in $(V_{1-x}Cr_x)_2O_3$ system sandwiched between the two insulating phases (cf., Fig. 8) does not exhibit this type of universality.

Summarizing, we have demonstrated that a single band model of Hubbard (*2*) rationalizes the phase diagram and the equilibrium properties of the V_2O_3 systems. In other words, the Gutzwiller approach (*7, 8*) when generalized to nonzero temperatures (*9, 10*) forms a starting basis for rationalization of the data for pure Ti-, Cr-, and vacancy-doped V_2O_3. The scheme presented here is based on the notion that the electronic transitions observed in these systems are driven by electron–electron repulsive interactions which are comparable to their kinetic energy. The spectacular predictions of the theory are discontinuous nature of the transitions, the reentrant metallic behavior at high temperature, and a large (and equal) enhancement of the specific heat and the magnetic susceptibility in the metallic phase close to the localization. All observed I → M and M → I transitions can be regarded as an example of Mott transition (*31*). In this way, the present theory resolves a long standing problem why the Mott transition AFI → PM in $(V_{1-x}Cr_x)_2O_3$ is accompanied by an "anti-Mott" transition PM → PI and still followed by another PI → PM′ transformation of localization of the electrons in the lower Hubbard subband (or in the Mott insulator) in the situation of the half-filled band configuration.

8. Concluding Remarks

The problem of electron localization in a crystalline material as induced by Coulomb interactions has been approached from three distinct directions. First, in his papers Mott (*32*) determined a critical interatomic separation below which the screening of nuclear charges is sufficiently strong to prevent the formation of hydrogenic like bound states in a solid. The criterion for the metal–insulator transition is $n^{1/3}a_H > 0.25$, where n is the carrier concentration and $a_H = \hbar\varepsilon/Me^2$ is the effective radius of hydrogeniclike 1s state in a medium with dielectric constant ε. This criterion of localization proved to be very successful for the description of heavily doped semiconductors such as Si : P. Second approach has been developed by Hubbard (*2*) who considered the narrow band model bearing his name; using a Green function technique he was able to show that for a critical ratio $U/W \sim 1$ a system with a half-filled narrow band splits into two subbands as shown in Fig. 1. The third approach was initiated by Gutzwiller (*7*) and elaborated in detail for $T = 0$ by Brinkman and Rice (*8*) in which the band is strongly narrowed with growing U/W: at $U = U_c$

the electrons become localized since their effective mass m^* diverges. It is not clear as yet how to relate the Hubbard and Gutzwiller–Brinkman–Rice pictures (Figs. 1 and 2). The Gutzwiller approach and its extension (*10*) have been discussed in detail in the present review since the invoked quasiparticle picture permits the generalization of the theory to nonzero temperatures (*9, 10*).

It must be emphasized that in the approach reviewed here the phase boundary for the discontinuous M → I transition at $T > 0$ is determined through a (free) energy balance of phases involved. At $T = 0$ the PM → PI transition is continuous; therefore consideration of the screening divergence (*8, 33*) can be applied to determine the stability limit for the metallic phase in this case.

The discussion of the metal–insulator transition for V_2O_3 system starting from the Hubbard model does not take into account important factors such as the coupling of the electron system to the lattice, the orbital degeneracy of the 3*d* states involved, and the disorder associated with the Ti, Cr substitutions or oxygen excess. The coupling to the lattice is important since there is a large volume change associated with the low temperature transitions and a remarkable hysteretic behavior accompanied the discontinuous transition (*19*). Hence, the theoretical model described above should be regarded as reproducing the main qualitative features of the observed effects. One feature should become clear: the volume changes and the observed hysteresis (*19*) are regarded as effects concomitant to the localization–delocalization transition induced by electron correlations.

One should also mention that an alternative approach based on a functional integration scheme (*34*) and coherent potential approximation (*35*) have been devised which provide phase diagrams similar to ours, except for the absence of the reentrant metallic behavior. However, the phase boundaries in those models are continuous, in disagreement with experiment for V_2O_3 system. The reader interested in a detailed discussion of those models is referred to Ref. (*36*).

Acknowledgments

This paper is dedicated to friend and co-worker George Honig, as part of a Festschrift in his honor. I am grateful to George for stressing the complexity of the "V_2O_3 problem," and for the countless discussions on the subject. I also express my gratitude to two students: Prakash Gopalan for cooperation on electron states in a magnetic field and M. P. Anantram for discussions on the Landau theory of Fermi liquids. The work was supported by the Superconductivity Center at Purdue University.

References

1. N. F. MOTT, *Proc. Phys. Soc. London A* **62,** 416 (1949); for review, see N. F. MOTT, "Metal–Insulator Transitions," Taylor & Francis. London (1974).
2. J. HUBBARD, *Proc. R. Soc. A* **281,** 401 (1964).
3. For a recent review, see P. W. ANDERSON, *in* "Frontiers and Borderlines in Many-Particle Physics" (R. A. Broglia and J. R. Schrieffer, Eds.), North-Holland, Amsterdam (1988).
4. P. W. ANDERSON, *Phys. Rev.* **115,** 2 (1959); also in *Solid State Phys.*, **14,** 99 (1963).
5. For review, see, e.g., B. H. BRANDOW, *Adv. Phys.* **26,** 651 (1977).
6. J. SPAŁEK AND A. M. OLEŚ, *Physica B* **86–88,** 375 (1977); K. A. CHAO, J. SPAŁEK, AND A. M. OLEŚ, *J. Phys. C* **20,** 27 (1977); J. SPAŁEK, A. M. OLEŚ, AND K. A. CHAO, *Phys. Status Solidi B* **108,** 329 (1981).
7. M. C. GUTZWILLER, *Phys. Rev. Lett.* **10,** 159 (1963); *Phys. Rev. 137,* A1726 (1965).
8. W. F. BRINKMAN AND T. M. RICE, *B2,* 4302 (1971); T. M. RICE AND W. F. BRINKMAN, *in* "Critical Phenomena in Alloys, Magnets and Superconductors" (R. E. Mills, E. Ascher, and R. Jaffee, Eds.), p. 593, McGraw–Hill, New York (1971).
9. J. SPAŁEK, A. M. OLEŚ, AND J. M. HONIG, *Phys. Rev. B* **28,** 6802 (1983).
10. J. SPAŁEK, A. DATTA, AND J. M. HONIG, *Phys. Rev. Lett.* **59,** 728 (1987); J. SPALEK, M. KOKOWSKI, AND J. M. HONIG, *Phys. Rev. B* **39,** 4175 (1989).
11. J. SPALEK AND P. GOPALAN, *Phys. Rev. Lett.* **64,** 2823 (1990), and to be published.
12. For a lucid discussion, see V. Z. VULOVIĆ AND E. ABRAHAMS, *Phys. Rev. B* **36,** 2614 (1987).

13. L. D. LANDAU, *Zh. Eksp. Teor. Fiz.* **30,** 1058 (1956); *Sov. Phys.-JETP* **3,** 920 (1957); for review see A. A. ABRIKOSOV AND I. M. KHALATNIKOV, *in* "Rep. Prog. Phys.," Vol. XXII, p. 329 (1959).
14. P. W. ANDERSON AND W. F. BRINKMAN, *in* "The Physics of Liquid and Solid Helium" (K. H. Benemann and J. B. Ketterson, Eds.), Part II, p. 177, Wiley, New York (1978).
15. D. VOLLHARDT, *Rev. Mod. Phys.* **56,** 99 (1984).
16. For a review of electron gas properties for $T \to 0$, see A. H. WILSON, "The Theory of Metals" pp. 14 and 133, Cambridge Univ. Press, London/New York, (1958).
17. J. W. RASUL AND T. LI, *J. Phys. C* **21,** 5119 (1988); T. LI, P. WÖLFLE, AND P. J. HIRSCHFELD, *Phys. Rev. B* **40,** 6817 (1989).
18. For a review of metal–insulator transition in $(V_{1-x}Cr_x)_2O_3$, see D. B. MCWHAN, A. MENTH, AND J. P. REMEIKA, *J. Phys. (Paris)* **32,** Colloque C1, 1079 (1971); N. F. MOTT, "Metal–Insulator Transitions," Taylor & Francis, London (1974) and references therein.
19. Reentrant metallic behavior has been discussed in H. KUWAMOTO, J. M. HONIG, AND I. APPEL, *Phys. Rev. B* **22,** 2626 (1980).
20. J. SPALEK, A. DATTA, AND J. M. HONIG, *Phys. Rev. B* **33,** 4891 (1986); J. SPALEK, J. M. HONIG, M. ACQUARONE, AND A. DATTA, *J. Magn. Magn. Mater.* **54–57,** 1047 (1986).
21. K. A. CHAO, *Solid State Commun.* **14,** 525 (1974).
22. J. M. LUTTINGER, *Phys. Rev.* **119,** 1153 (1960).
23. J. M. HONIG AND J. SPAŁEK, *Proc. Indian Nat. Sci. Acad. Part A* **52,** 232 (1986); A. DATTA, Ph.D. thesis, Purdue University (1988) unpublished.
24. T. OGAWA, K. KANDA, AND T. MATSUBARA, *Prog. Theor. Phys.* **53,** 614 (1975).
25. D. B. MCWHAN, A. MENTH, J. P. REMEIKA, W. F. BRINKMAN, AND T. M. RICE, *Phys. Rev. B* **7,** 1920 (1973).
26. The results in Fig. 17 are a compilation of the Bell group data taken from Ref. (*26*), and from D. B. MCWHAN AND J. P. REMEIKA, *Phys. Rev. Lett.* **27,** 941 (1971); D. B. MCWHAN AND T. M. RICE, *Phys. Rev. Lett.* **22,** 887 (1969).
27. Y. UEDA, K. KOSSUGE, S.KACHI, AND T. TAKADA, *J. Phys. (Paris) C* **40(2),** 275 (1979); Y. UEDA, K. KOSUGE, AND S. KACHI, *J. Solid State Chem.* **31,** 171 (1980).
28. T. F. ROSENBAUM, this Festschrift.
29. S. A. SHIVASHANKAR AND J. M. HONIG, *Phys. Rev. B* **28,** 5695 (1983).
30. S. A. CARTER, J. YANG, T. F. ROSENBAUM, J. SPAŁEK, AND J. M. HONIG, submitted to *Phys. Rev. B.*
31. The idea that V_2O_3 systems undergo a Mott transition was coined in D. B. MCWHAN, T. M. RICE, AND J. P. REMEIKA, *Phys. Rev. Lett.* **23,** 1384 (1969).
32. N. F. MOTT, *Philos. Mag.* **6,** 287 (1961).
33. N. F. MOTT, *in* "The Metallic and Nonmetallic States of Matter," (P. P. Edwards and C. N. R. Rao, Eds.), p. 1, Taylor & Francis, London (1985).
34. M. CYROT, *Philos. Mag.* **25,** 1031 (1971); Y. KAKEHASHI AND H. HASEGAWA, *Phys. Rev. B* **37,** 7777 (1988) and references therein.
35. E. N. ECONOMU, C. T. WHITE, AND R. R. DE MARCO, *Phys. Rev. B* **18,** 3946 (1978); C. T. WHITE AND E. N. ECONOMU, *Phys. Rev. B* **15,** 3742 (1977); C. T. WHITE AND E. N. ECONOMU, *Phys. Rev. B* **18,** 3959 (1978).
36. T. V. RAMAKRISHNAN, *in* "The Metallic and Nonmetallic States of Matter" (P. P. Edwards and C. N. R. Rao, Eds.), p. 23, Taylor & Francis, London (1985).